A Passive Circularly Polarized Van Atta Reflector For Vehicle Radar Applications

Zhuo-Wei Miao, *Student Member, IEEE*, Zhang-Cheng Hao, *Senior Member, IEEE*, and Quan Yuan

***Abstract*—This letter proposes a planar passive circularly polarized (CP) retrodirective antenna (RDA) array for vehicle radar applications. Different than the linearly polarized RDA arrays, the retrodirective signal generated by the CP RDA arrays can easily be extracted due to the orthogonal polarized character of the scattering and retrodirective signals. Circular polarization is achieved by a substrate integrated waveguide cavity-backed antenna. Moreover, the low-loss and nondispersive substrate integrated coaxial lines are employed as the feeding networks to expand the operating bandwidth for the large array. Measured results of bistatic and monostatic radar cross section verify the designed prototype, showing that the CP RDA array covers a scan angle of at least ±30° from boresight without interference by sidelobes. The measured bandwidth of the retrodirective property is 24.85–25.45 GHz. The capability of CP retrodirectivity ensures that the proposed RDA array is a good candidate for short-range vehicle radio equipment.**

***Index Terms*—Circular polarization (CP), radar cross section (RCS), retrodirective antenna (RDA), substrate integrated coaxial line (SICL), Van Atta array, vehicle application.**

I. Introduction

RETRODIRECTIVE self-steering arrays have drawn increasing attention in modern space and communication system since 1959 [1]–[5]. Compact and planar topologies have been highly desired in modern communication systems. Thin and flexible retrodirective patch antenna arrays are adopted for their radar cross section (RCS) response enhancement [4], [6]. Due to the characteristics of low cost and high Q-factor, substrate integrated waveguide (SIW)-based retrodirective antenna (RDA) arrays have also been a popular candidate [7], [8]. In addition, amplifiers or mixers are added in the transmission lines to eliminate fading effects of multipath propagation and improve the signal-to-noise ratio [2], [9]. High cost and complex design process are inevitable although the performance is improved by using the active devices. Consequently, passive RDA arrays continue to be extraordinarily valuable in low-cost applications.

The reflected or scattering waves keep the same polarization character if the incident waves are linearly polarized (LP). However, the retrodirective signal is difficult to be extracted from the total bistatic RCS (BRCS) response because the scattering and retrodirective signals are mixed. The strategy of polarization rotation of reradiated fields is proposed in [7] and [10]. However, this strategy requires that the transmitting and receiving antennas should have different polarizations, and leads to increased cost and size of the system. To this end, the circularly polarized (CP) Van Atta antenna is a competitive choice for the RDA system. In the CP system, the reflected or scattering waves are orthogonal to the incident waves, and the retrodirective waves are designed with the same polarization of the incident waves. Consequently, the transmitting and receiving antennas of the RDA system can share the same antenna to improve the compactness and reduce the cost of the system. Nevertheless, most of the reported Van Atta reflectors are excited by an LP plane wave, and research on CP RDA arrays is rare [11].

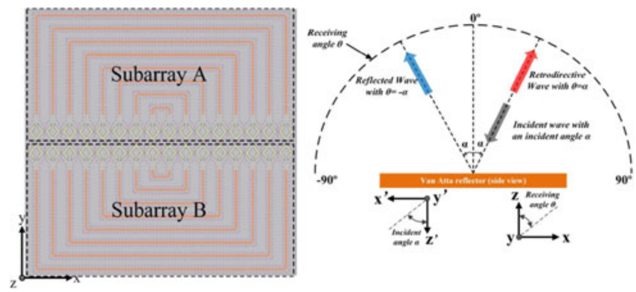

Fig. 1. Configuration of the proposed CP Van Atta reflector with definition of the coordinates.

As a potential application of the RDA arrays, the short-range vehicle-borne radar has attracted much attention recently [7]. The Ministry of Industry and Information Technology of China has granted the frequency band of 24.25–26.65 GHz for the vehicle radar recently. In this letter, a novel passive CP RDA array with good selectivity and moderate bandwidth of retrodirective behavior has been first designed in that frequency range. The radiation unit and the proposed Van Atta reflector are presented in Section II with simulated results. Experiment results of the bistatic and monostatic RCS responses are shown in Section III to verify the designed prototype, and conclusions are drawn in Section IV.

II. Design of the CP Van Atta Array

As is shown in Fig. 1, antenna elements, i and $2N+1-i$, are equidistant from RDA array center. The electrical lengths of feeding networks (FNs) have a difference of multiple wavelengths at the center operating frequency. The bandwidth of

Manuscript received May 2, 2017; revised May 30, 2017; accepted May 31, 2017. Date of publication June 2, 2017; date of current version August 7, 2017. This work was supported by the National Natural Science Foundation of China under Grant 61471118. *(Corresponding author: Zhang-Cheng Hao.)*

The authors are with the State Key Laboratory of Millimeter-Waves, School of Information Science and Engineering, Southeast University, Nanjing 210096, China (e-mail: zchao@seu.edu.cn; zwmiao@seu.edu.cn; yq1989@seu.edu.cn).

Color versions of one or more of the figures in this letter are available online at http://ieeexplore.ieee.org.

Digital Object Identifier 10.1109/LAWP.2017.2711492

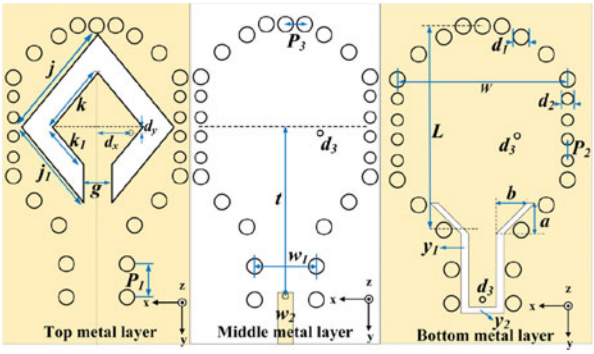

Fig. 2. Configuration of the proposed CP antenna unit (shaded color for metal surface and white color for substrate). Two 0.508-mm Taconic TLY-5 ($\varepsilon_r = 2.2$) are bonded together.

TABLE I
GEOMETRICAL PARAMETERS OF THE PROPOSED ANTENNA ELEMENT (mm)

j	6.34	j_1	5.16	W_2	1.5
k	3.74	k_1	2.56	W	8.8
W_s	1.29	G	1.5	A	1.6
d_x	1.8	d_y	0.32	y_1	0.4
P_1	1.75	P_2	1.1	T	8.8
P_3	1	d_1	0.32	L	10.55
d_2	0.6	d_3	0.3	B	1.6
d_4	0.3	W_1	3.2	y_2	0.3

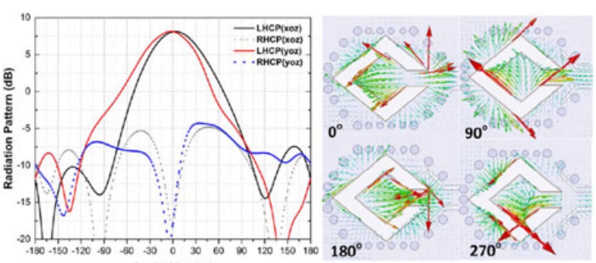

(a) (b)

Fig. 3. (a) Radiation patterns at 25.45 GHz. (b) Current distribution at different phase at 25.45 GHz.

retrodirective property is determined by radiation elements and the FNs, especially the later ones. This is because it is very difficult for large planar arrays to keep the same electrical length in a wide frequency band between antenna pairs. Hence, low dispersive FNs are desired for reducing the feeding phase variations of the antenna pairs.

A. CP Radiation Unit

Two-dimensioanl configuration of the radiation unit is presented in Fig. 2. The CP wave is generated by a combination of a diamond ring slot etched on the SIW top surface and a shorting via, as in [12]. The initial size of the SIW cavity and length of the diamond ring can be evaluated by the formulas in [13, (1)]. The location of the shorting via greatly influences the CP performance. After a full-wave simulation, the final dimensions of the element antenna are listed in Table I. Simulated results of the proposed CP unit are shown in Fig. 3 and Table II.

TABLE II
SIMULATED RESULTS OF THE RADIATION UNIT

15-dB return loss (S_{11})	24.6–27.3 GHz (10.6%)
3-dB axial ratio (AR)	24.5–26.7 GHz (8.64%)
Peak Gain (dBic)	8.8

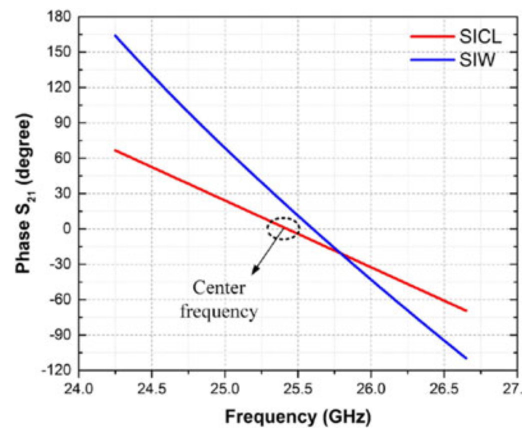

Fig. 4. Phase responses for a specified length of SICL and an SIW transmission line with the same length from 24.25 to 26.65 GHz.

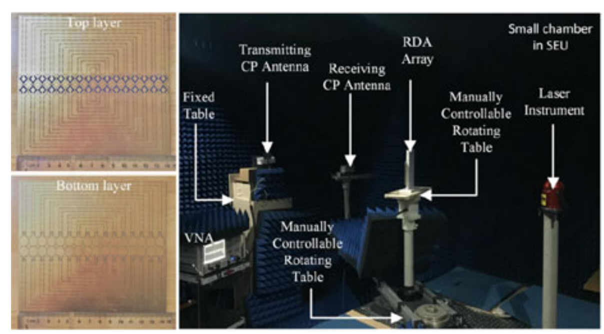

Fig. 5. Photographs of the fabricated CP RDA array and the measurement setup in a chamber.

B. CP RDA Array With Simulated Results

As explained above, the transmitting lines severely limit the overall performance of the RDA arrays. When the number of antenna pairs increases, the phase error between the longest and shortest transmitting lines increases significantly, which results in a relatively narrower bandwidth. The substrate integrated coaxial lines (SICLs), which are less sensitive to design inaccuracies, are adopted as the transmitting structures in this work [14]. It can moderately broaden the bandwidth compared to some dispersive structures (SIW) used in the RDA system [7], [8]. The proposed FNs in the Van Atta reflector are shown in Fig. 1. Each connecting line has the same bend geometry so that only the length difference of the straight segment needs to be taken into consideration. To satisfy the identical phase delay at 25.45 GHz, a 30.812-mm length difference between adjacent feeding lines is adopted for SICLs, and the simulated phase difference response is shown in Fig. 4(d), where a maximum phase error of 68° can be found in the frequency range (24.25–26.65 GHz).From Fig. 4, the simulated phase responses

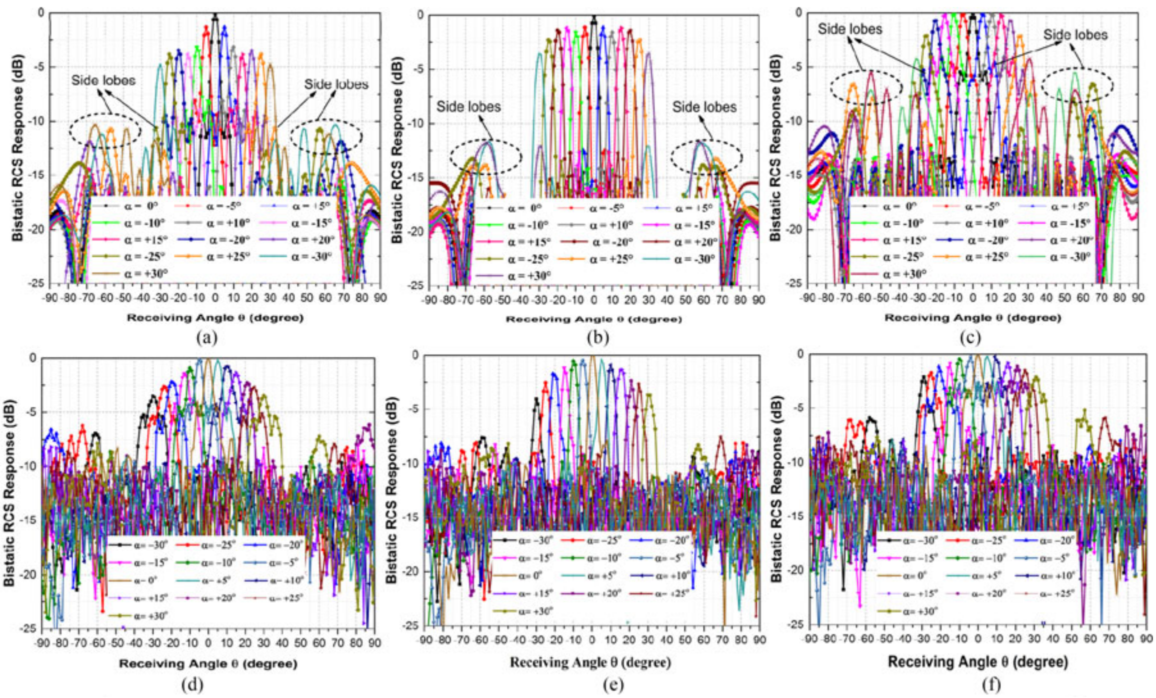

Fig. 6. Simulated results of normalized BRCS responses at (a) 25.15, (b) 25.45, and (c) 25.75 GHz. Measured results of normalized BRCS responses at (d) 24.85, (e) 25.15, and (f) 25.45 GHz.

of an SIW transmission line with the same length as a comparison show the low dispersion characteristic of SICL structure as the connecting lines used in the proposed RDA design.

The fabricated CP RDA array centered at 25.45 GHz with a size of 14.3×13.27 cm^2 is presented in Fig. 5. To achieve high gain and narrow principal half-power beamwidth, the RDA array contains two subarrays with 32 radiation units. For a subarray, the 16 radiation units are placed in a row with the separation distance $d_i = 8.8$ mm between the centers of adjacent elements for lower sidelobes. All the antenna units can both receive and transmit left-hand circularly polarized (LHCP) waves. Due to the orthogonal polarizations, the right-hand circularly polarized (RHCP) reflected wave and the LHCP retrodirective wave are separated automatically.

In this letter, the scan ability of the RDA array includes scan range, selectivity, and retrodirective bandwidth. For a better view of the scan ability, BRCS responses are calculated by using CST software with an LHCP plane wave excitation. The incident angle changes from $-30°$ to $30°$ by the step of $5°$. The simulated bistatic results in Fig. 6(b), which are normalized with their peak value, show that the proposed Van Atta reflector covers a scan range of at least $\pm 30°$ from boresight (see z-axis in Fig. 1) without interference by sidelobes at the center frequency. It can be predicted in Fig. 6(b) that the sidelobes will move toward the main lobe and give rise to pointing error if the incident angle continues to increase. In addition, the top layer of the proposed RDA array can be viewed as a metal reflector, which has a larger size than the radiation elements. Hence, the power level of RHCP monostatic RCS (MRCS) becomes strong near zero degree and much higher than that of the retrodirective signal. The MRCS responses in incident direction ($\theta = \alpha$) are provided in Fig. 7(a). The black line represents the MRCS response of LHCP retrodirective waves, and the red line represents the corresponding value of RHCP waves when $\theta = \alpha$. It can be concluded that the RCS value of LHCP wave is about 10 dB higher than the RCS value of RHCP wave on the average. Fig. 6(a) and (c) presents the simulated results of normalized BRCS response at 25.15 and 25.75 GHz, respectively. A moderate bandwidth of retrodirective property with high selectivity is achieved with no pointing error.

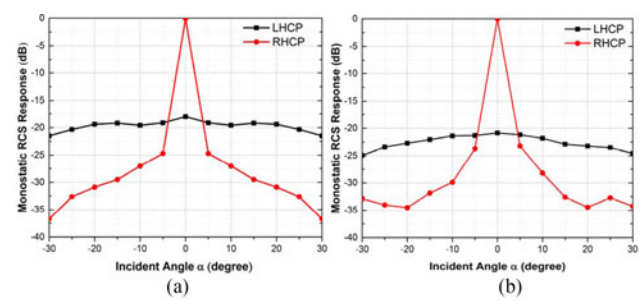

Fig. 7. (a) Simulated monostatic RCS responses of the RDA array at 25.45 GHz. (b) Measured monostatic RCS responses of the RDA array at 25.15 GHz (center frequency of measured results).

III. Experimental Results and Discussion

To experimentally show the retrodirective property of the RDA array, the measurement setup is shown in Fig. 5. It is composed of K-band CP antennas, a manually rotating table with the RDA array, an electronically controllable rotating table, and a network analyzer connected with a laptop.

The prototype is placed on the manually controllable rotating table with angle marks to obtain different incident angles. Because it is impossible to place the transmitting and receiv-

TABLE III
COMPARISONS AMONG REFERRED RDA ARRAYS AND THIS WORK

Reference	This work	[7]	[8]	[9]	[11]
Polarization	CP	LP	LP	LP	CP
Unit number	32	16	32	64	4
Structure of FN	shielded	shielded	shielded	open	open
Scan ability	±30° for BRCS/10 dB enhancement for MRCS	±17° for BRCS	11 dB enhancement for MRCS	20 dB enhancement for MRCS	±60° for BRCS
Center frequency	25.15 GHz	79 GHz	35 GHz	26 GHz	5.8 GHz
BW for retrodirectivity	2.4% (24.85–25.45 GHz)	Single point at 79 GHz	Single point at 35 GHz	Single point at 26 GHz	≥30% (5–7 GHz)
Active/Passive	Passive	Passive	Passive	Active	Active
Selectivity	Good	Good	/	/	moderate

ing antennas on the same horizontal plane due to the mutual shielding effect, which is caused by the transmitting or receiving antenna and results in a depression at the direction of retrodirective signal, the aperture planes of the transmitting and receiving antennas are set at the same vertical plane when the receiving LHCP antenna rotates at the retrodirective direction. In addition, the receiving LHCP antenna is placed at the distance 1.3 m away from the RDA array, which satisfies the far-field condition calculated by the radiation aperture. Furthermore, all the measurements are calibrated carefully by the laser instrument and spirit level for many times. Finally, the total BRCS responses are achieved to show the retrodirective property, as well as the retrodirective bandwidth.

The scan ability of the Van Atta reflector of all the frequency points can be obtained by the Keysight PNA Network Analyzer at one time, as is shown in Fig. 6(d)–(f). For a better view of the scan ability, all the BRCS responses with different incident angles ($-30°$ to $+30°$) are normalized with their peak values. The best results of retrodirective property are obtained at 25.15 GHz. The rising sidelobes, which limit the scan angles, also can be observed in Fig. 6. Moreover, the bandwidth of the retrodirective property can be measured from the BRCS responses of all the frequency points. The measured results of BRCS responses at 24.85 and 25.45 GHz are presented in Fig. 6(d) and (f), respectively. As the frequency of the incident wave deviates from the center frequency (25.15 GHz), the power level of sidelobe near the retrodirective beam will increase and cause a pointing error. If the frequency of incident wave is out of the range of 24.85–25.45 GHz, the retrodirective property cannot be accepted due to the unequal phase delay.

To show the RCS enhancement, an RHCP antenna is adopted as the receiving antenna to achieve the RHCP RCS responses in the direction of retrodirectivity ($\theta = \alpha$). The monostatic LHCP RCS responses of the proposed RDA array, shown in Fig. 7(b), are measured by manually rotating the RDA array when the receiving antenna is set in the direction of retrodirectivity ($\theta = \alpha$). All the monostatic RCS responses are normalized to the peak value of monostatic RHCP RCS response. It can be seen that about 10 dB enhancement of the monostatic RCS response is achieved, so the Van Atta array has great potential for vehicle radar applications. Last but not the least, there is a 0.3-GHz frequency shifting between simulation and measurement for retrodirective property. This is most likely caused by the tolerance of manufacture in the connecting networks.

Some up-to-date RDA arrays have been summarized and compared to the proposed Van Atta reflector, as shown in Table III. The proposed Van Atta reflector is one of few passive RDA arrays that can realize circular polarization with good performance. It covers a wide scan angle and has a moderate bandwidth of retrodirective property. Hence, it is promising for short-range vehicle radio applications.

IV. CONCLUSION

In this letter, a passive CP Van Atta reflector is investigated for vehicle radar application. The design procedure is presented, and a prototype of 32 elements is fabricated. Measured and simulated results of the fabricated prototype are in good agreement. The proposed Van Atta array covers a scan angle of $\pm 30°$ from boresight without interference by sidelobes and has a moderate bandwidth of retrodirective property. The retrodirective signal can be separated with the reflected one because of the polarization rotation of the reflected wave if both the transmitting and receiving antennas are LHCP in practical short-range wireless communication.

REFERENCES

[1] L. C. Van Atta, “Electromagnetic reflector,” U.S. Patent 2 908 002, Oct. 1959.
[2] E. L. Gruenberg and C. M. Johnson, “Satellite communication relay system using a retrodirective space antenna,” *IEEE Trans. Antennas Propag.*, vol. AP-12, no. 2, pp. 215–223, Mar. 1964.
[3] S. N. Andre and D. Leonard, “An active retrodirective array for satellite communications,” *IEEE Trans. Antennas Propag.*, vol. AP-12, no. 2, pp. 181–186, Mar. 1964.
[4] J. G. D. Hester and M. M. Tentzeris, “Inkjet-printed flexible mm-wave van-atta reflectarrays: A solution for ultralong-range dense multitag and multisensing chipless RFID implementations for IoT smart skins,” *IEEE Trans. Microw. Theory Techn.*, vol. 64, no. 12, pp. 4763–4773, Dec. 2016.
[5] D. A. Williams, “Millimeter wave radars for automotive applications,” in *IEEE MTT-S Int. Microw. Symp. Dig.*, pp. 721–724, Jun. 1992.
[6] P. Hallbjörner and S. Cheng, “Improvement in 77-GHz radar cross section of road work jacket and side screen by use of planar flexible retrodirective reflectors,” *IEEE Antennas Wireless Propag. Lett.*, vol. 12, pp. 1085–1088, 2013.
[7] H. Zhou *et al.*, “A retrodirective antenna array with polarization rotation property,” *IEEE Trans. Antennas Propag.*, vol. 62, no. 8, pp. 4081–4088, Aug. 2014.
[8] A. A. M. Ali, H. B. El-shaarawy, and H. Aubert, “Millimeter-wave substrate integrated waveguide passive Van Atta reflector array,” *IEEE Trans. Antennas Propag.*, vol. 61, no. 3, pp. 1465–1470, Mar. 2013.
[9] J. A. Vitaz, A. M. Buerkle, and K. Sarabandi, “Tracking of metallic objects using a retro-reflective array at 26 GHz,” *IEEE Trans. Antennas Propag.*, vol. 58, no. 11, pp. 3539–3544, Nov. 2010.
[10] M. Fujita and S. Nakamuar, “A polarization-rotating Van Atta array reflector and its application to polarimetric radar calibration,” in *Proc. Int. Symp. IEEE Geosci. Remote Sens.*, Sep. 2004, vol. 3, pp. 1746–1749.
[11] L. Chiu, Q. Xue, and C. H. Chan, “A Wideband circularly-polarized active van atta retrodirective transponder with information carrying ability,” in *Proc. Int. Conf. IEEE Asia-Pacific Microw.*, Dec. 2006, pp. 231–234.
[12] J. Lacik, “Circularly polarized SIW square ring-slot antenna for X-band applications,” *Microw. Opt. Technol. Lett.*, vol. 54, pp. 2590–2594, Nov. 2012.
[13] Z. C. Hao and X. M. Liu, “Planar high gain circularly polarized element antenna for array applications,” *IEEE Trans. Antennas Propag.*, vol. 63, no. 5, pp. 1937–1948, May 2015.
[14] F. Gatti, M. Bozzi, L. Perregrini, K. Wu, and R. G. Bosisio, “A novel substrate integrated coaxial line (SICL) for wide-band applications,” in *Proc. 36th Eur. Conf. Microw.*, Manchester, U.K., Sep. 2006, pp. 1614–1617.